

Differential Regulation of Skeletal Muscle L-Type Ca^{2+} Current and Excitation-Contraction Coupling by the Dihydropyridine Receptor β Subunit

Maryline Beurg,* Manana Sukhareva,* Chris A. Ahern,* Matthew W. Conklin,* Edward Perez-Reyes,# Patricia A. Powers,[§] Ronald G. Gregg,[¶] and Roberto Coronado*

*Department of Physiology, University of Wisconsin School of Medicine, Madison, Wisconsin 53706; #Department of Physiology, Loyola University Medical Center, Maywood, Illinois 60153; [§]Biotechnology Center, University of Wisconsin, Madison, Wisconsin 53706; and

[¶]Department of Biochemistry, University of Louisville, Louisville, Kentucky 40202 USA

ABSTRACT The dihydropyridine receptor (DHPR) of skeletal muscle functions as a Ca^{2+} channel and is required for excitation-contraction (EC) coupling. Here we show that the DHPR β subunit is involved in the regulation of these two functions. Experiments were performed in skeletal mouse myotubes selectively lacking a functional DHPR β subunit. These β -null cells have a low-density L-type current, a low density of charge movements, and lack EC coupling. Transfection of β -null cells with cDNAs encoding for either the homologous β_{1a} subunit or the cardiac- and brain-specific β_{2a} subunit fully restored the L-type Ca^{2+} current (161 ± 17 pS/pF and 139 ± 9 pS/pF, respectively, in 10 mM Ca^{2+}). We compared the Boltzmann parameters of the Ca^{2+} conductance restored by β_{1a} and β_{2a} , the kinetics of activation of the Ca^{2+} current, and the single channel parameters estimated by ensemble variance analysis and found them to be indistinguishable. In contrast, the maximum density of charge movements in cells expressing β_{2a} was significantly lower than in cells expressing β_{1a} (2.7 ± 0.2 nC/ μF and 6.7 ± 0.4 nC/ μF , respectively). Furthermore, the amplitude of Ca^{2+} transient measured by confocal line-scans of fluo-3 fluorescence in voltage-clamped cells were 3- to 5-fold lower in myotubes expressing β_{2a} . In summary, DHPR complexes that included β_{2a} or β_{1a} restored L-type Ca^{2+} channels. However, a DHPR complex with β_{1a} was required for complete restoration of charge movements and skeletal-type EC coupling. These results suggest that the β_{1a} subunit participates in key regulatory events required for the EC coupling function of the DHPR.

INTRODUCTION

The dihydropyridine receptor (DHPR) of skeletal muscle is a heterotetramer composed of a pore-forming α_{1S} subunit in tight association with β_{1a} , $\alpha_2\text{-}\delta$, and γ subunits. The β subunit is an ~55- to 65-kDa cytoplasmic protein that interacts with a cytoplasmic loop in the α_1 subunit (Pragnell et al., 1994); β isoforms are encoded by four different genes and several splice variants have been described. The predominant isoform of skeletal muscle is β_{1a} (Ruth et al., 1989; Powers et al., 1992) whereas that of cardiac muscle is the β_{2a} isoform (Perez-Reyes et al., 1992). Numerous properties of L-type Ca^{2+} channels are modulated by the β subunit as determined by transient expression in frog oocytes and heterologous cell lines. Coexpression of cardiac or brain α_1 isoforms with β_{2a} or β_{1a} resulted, in most cases, in faster Ca^{2+} currents with a higher current density (Singer et al., 1991; Wei et al., 1991; Lacerda et al., 1991; Perez-Reyes et al., 1992; Lory et al., 1992; Hullin et al., 1992; Nishimura et al., 1993; Stea et al., 1993; Castellano et al., 1993; Olcese et al., 1994; De Waard et al., 1994; Perez-Garcia et al., 1995; Quin et al., 1996; Tareilus et al., 1997).

In addition, β subunits facilitate gating of the Ca^{2+} channel by increasing coupling between charge movement and pore opening (Neely et al., 1993; Olcese et al., 1996; Noceti et al., 1996) although this is not a general feature of all combinations of α_1 and β subunits (Josephson and Varadi, 1996; Kamp et al., 1996).

The DHPR of skeletal muscle triggers excitation-contraction (EC) coupling. EC coupling is initiated by charge movements in the DHPR complex and activation of these charges does not necessarily lead to activation of the L-type Ca^{2+} current (Pizarro et al., 1988). Kinetic steps controlling both cellular functions of the DHPR, namely Ca^{2+} currents and charge movements associated to EC coupling, have been clearly distinguished by a variety of experimental protocols (Lamb, 1992). However, the mechanisms that regulate the expression of the L-type Ca^{2+} current and charge movements have remained elusive. Expression of the α_{1S} isoform in the α_{1S} -deficient dysgenic skeletal muscle myotube supports the premise that both functions of the DHPR are carried out by the same population of DHPRs. In this expression system, the recovery of the L-type Ca^{2+} current parallels the recovery of charge movements and the recovery of EC coupling (Tanabe et al., 1988). In more recent years, the involvement of the DHPR β subunit in expression of L-type Ca^{2+} currents, charge movements, and EC coupling has been examined in β -null cells from knockout mice carrying a null mutation in the β_1 gene (Gregg et al., 1996). Intercostal β -null myotubes fail to contract in response to electrical stimulation despite the presence of

Received for publication 28 September 1998 and in final form 5 January 1999.

Address reprint requests to Roberto Coronado, Department of Physiology, University of Wisconsin, 1300 University Ave., Madison, WI 53706. Tel.: 608-263-7487; Fax: 608-265-5512; E-mail: coronado@physiology.wisc.edu.

© 1999 by the Biophysical Society

0006-3495/99/04/1744/13 \$2.00

normal action potentials, a normal Ca^{2+} storage capacity, and normal caffeine-sensitive Ca^{2+} release. Strube et al., 1996 showed that β -null cells have a low density of charge movements and do not generate Ca^{2+} transients in response to depolarization. Evidently, β -null cells fail to transduce depolarization into Ca^{2+} release from the sarcoplasmic reticulum due either to a low density of DHPRs or the specific absence of β_{1a} from the DHPR. In these cells, the expression of β_{1a} , the missing endogenous β subunit, results in a quantitative recovery of the L-type Ca^{2+} current density of normal cells, the intramembrane charge movement density, the amplitude and voltage dependence of intracellular Ca^{2+} transients, and Ca^{2+} entry-independent skeletal type EC coupling, all within 3 to 6 days after cDNA transfection (Beurg et al., 1997). These results have clearly demonstrated that a DHPR complex that includes β_{1a} is required for the functional expression of L-type Ca^{2+} channels and charge movements associated to EC coupling.

In the present report we investigated whether a nonskeletal muscle DHPR β isoform such as β_{2a} could substitute for β_{1a} in the recovery of the L-type Ca^{2+} current, EC coupling, or both when expressed in β -null myotubes. Whereas β_{2a} fully restored L-type Ca^{2+} currents, it could not entirely restore EC coupling. Thus the Ca^{2+} channel and EC coupling functions of the DHPR are separately regulated by the DHPR β subunit. Part of these results appeared in abstract form (Beurg et al., 1998a).

MATERIALS AND METHODS

Primary cultures of mouse myotubes

Primary cultures were prepared from hindlimbs of 18-day-old mouse fetuses as described elsewhere (Beurg et al., 1997). Homozygotes for the β_1 -null mutation (*cchb1*^{-/-}) were recognized as described (Gregg et al., 1996). Controls, hereafter called normals, were either heterozygotes (*cchb1*^{+/-}) or wild type (*cchb1*^{+/+}). Dissected muscles were incubated for 9 min at 37°C in $\text{Ca}^{2+}/\text{Mg}^{2+}$ -free Hanks balanced salt solution (in mM) (136.9 NaCl, 3 KCl, 0.44 KH_2PO_4 , 0.34 NaHPO_4 , 4.2 NaHCO_3 , 5.5 glucose, pH 7.2) containing 0.25% (w/v) trypsin and 0.05% (w/v) pancreatin (Sigma, St. Louis, MO). Mononucleated cells were resuspended in plating medium containing 78% Dulbecco's modified Eagle's medium with low glucose (DMEM, Gibco BRL, Gaithersburg, MD), 10% horse serum (HS, Sigma), 10% fetal bovine serum (FBS, Sigma), 2% chicken embryo extract (CEE, Gibco) and plated on plastic culture dishes coated with gelatin at a density of $\sim 1 \times 10^4$ cells per dish. Cultures were grown at 37°C in 8% CO_2 . After the fusion of myoblasts (~ 7 days), the medium was replaced with a FBS-free medium (88.75% DMEM, 10% horse serum, 1.25% CEE) and cells were incubated in 5% CO_2 . All media contained 0.1% v/v penicillin and streptomycin (Sigma).

cDNA transfection

A full-length mouse β_{1a} and a full-length rabbit β_{2a} cDNA were separately subcloned into a pSG5 expression plasmid (Stratagene, La Jolla, CA) containing the early simian virus-40 (SV40) promoter. Cotransfection of the pSG5 expression plasmid and a separate marker plasmid encoding the T-cell membrane antigen CD8 was performed with the polyamine LT-1 (Panvera, Madison, WI). Cotransfected cells were recognized by incubation with CD8 antibody beads (Dynal, Oslo, Norway). Better than 95% of

cells expressing CD8 also expressed β_{1a} or β_{2a} as determined from the density of L-type Ca^{2+} currents.

Ca^{2+} current and charge movements

Whole-cell recordings were performed as described previously (Strube et al., 1996). We used an Axopatch 1D amplifier with a 50 M Ω feedback resistor or an Axopatch 200B (Axon Instruments, Foster City, CA). Linear capacitance and leak currents were compensated with an analog circuit or the circuit provided by the manufacturer, respectively. Effective series resistance was compensated up to the point of amplifier oscillation with the Axopatch circuit. The external solution was (in mM) 130 TEA methanesulfonate, 10 CaCl_2 , 1 MgCl_2 , 10^{-3} TTX, and 10 HEPES titrated with TEA(OH) to pH 7.4. The pipette solution consisted of (in mM) 140 cesium aspartate, 5 MgCl_2 , 0.1 EGTA (when Ca^{2+} transients were recorded), or 5 EGTA (all other recordings), and 10 MOPS titrated with CsOH to pH 7.2. Patch pipettes had a resistance of 2–5 M Ω when filled with the pipette solution. For recordings of charge movement, the external solution was supplemented with 0.5 mM CdCl_2 and 0.1 mM LaCl_3 to block the ionic Ca^{2+} currents. A prepulse protocol described elsewhere (Beurg et al., 1997) was used to measure the immobilization resistant component of charge movement. Voltage was first stepped from a holding potential of -80 mV or -120 mV to -20 mV for 1 s, then to -50 mV for 5 ms, then to test potential P for 25 ms, then to -50 mV for 30 ms, and finally to the -80 mV holding potential. Subtraction of linear components was assisted by a P/4 procedure following the pulse paradigm listed above. P/4 pulses were in the negative direction, had a duration of 25 ms, were separated by 500 ms, and were delivered from -80 mV. Currents were filtered with a low-pass Bessel filter at a corner frequency of 2 kHz and sampled at 200–250 μs per point. All experiments were performed at room temperature.

Variance analysis

The ensemble variance of whole-cell Ca^{2+} currents was estimated from the ensemble average of the squared difference between consecutive current records as described previously (Strube et al., 1998). A set of 50 pulses to $+20$ mV was delivered to the same cell at a rate of 1 pulse every 5 s from a holding potential of -40 mV. Test pulse duration and sampling frequency were 100 ms and 10 kHz, respectively. All records were low-pass filtered at 2 kHz at the moment of acquisition using an 8-pole analog Bessel filter. Amplifier gain was set at 5 mV/pA and the A/D resolution was 0.5 pA per bit. Pairs of consecutive records were subtracted in an overlapped manner to generate 49 difference records from which the ensemble variance was calculated. The resting variance was subtracted from the pulse variance, $\sigma^2(t)$, and the latter plotted against the mean pulse current, $I(t)$. The mean-variance relationship was fit by a nonlinear least-squares method according to

$$\sigma^2(t) = iI(t) - I^2(t)/N_F \quad (1)$$

where i is the single channel current and N_F is the number of functional channels activated by the voltage pulse. Up to 10 difference records in a set of 49 records were discarded from the analysis due to deterioration of the pipette seal resistance or excess of current rundown during the acquisition of one or both of the original pair of current records. These records were discarded without assumptions concerning the time course of the pulse variance as suggested by Heinemann and Conti (1992) and described elsewhere (Strube et al., 1998). Variance calculations were verified using pseudo-macroscopic ensemble currents generated by a single channel simulation program (CSIM, Axon Instruments).

Confocal fluorescence microscopy

Confocal measurements were performed as described elsewhere (Conklin et al., 1998). Cells were loaded with 4 μM fluo-3 acetoxymethyl (AM) ester (Molecular Probes, Eugene, OR) for 20 to 40 min at room tempera-

ture. Cells were viewed with an inverted Olympus microscope with a 20× objective (N.A. = 0.4) and an Olympus Fluoview confocal attachment (Melville, NY). The 488-nm spectrum line necessary for fluo-3 excitation was provided by a 5 mW argon laser. The laser power was attenuated to 20% with neutral density filters. The dimensions of the line-scan images were 512 pixels/line with a pixel size of 0.25 μm and 1000 lines/image. The z axis resolution was $\sim 0.8 \mu\text{m}$ and was estimated by imaging sub-resolution fluorescent beads (Molecular Probes). The line-scan rate was calibrated with a light-emitting diode and a voltage pulse from a digital pulse generator. The line-scan rate was 2.05 ms per 512-pixel line. The fluorescence intensity, F , was calculated by densitometric scanning of line-scan images and was averaged over the entire width of the cell. The fluorescence intensity, F_0 , was averaged in the same manner from areas of the same image before the voltage pulse. The fluorescence unit $\Delta F/F_0$ was constructed by subtracting unity from the ratio F/F_0 . A compressed 32-color table and an 8-pixel running average (smoothing) was applied to all images to highlight the Ca^{2+} transient. The pixel intensity as a function of time and space was obtained directly from the line-scan image with tools provided by National Institutes of Health-Image 1.6 (National Institutes of Health, Bethesda, MD). All experiments were performed at room temperature.

Chemicals

A 1-mg sample of fluo-3 AM (Molecular Probes) was dissolved in 1 ml of DMSO and kept frozen until use. Deionized glass-distilled water was used in all solutions. All salts were reagent grade. TTX was from Sigma Chemical Co. St. Louis, MO.

Curve-fitting

For each cell, the voltage dependence of charge movements (Q), Ca^{2+} conductance (G), and peak intracellular Ca^{2+} ($\Delta F/F_0$) was fitted according to a Boltzmann distribution

$$A = A_{\max}/(1 + \exp(-(V - V_{1/2})/k)). \quad (2)$$

A_{\max} was either Q_{\max} , G_{\max} , or $\Delta F/F_{0(\max)}$, $V_{1/2}$ is the potential at which $A = A_{\max}/2$, and k is the slope factor. The time constant, τ_1 , describing

activation of the Ca^{2+} current, was obtained from a fit of the pulse current at each voltage according to

$$I(t) = K[1 - (\exp(-t/\tau_1))]\exp(-t/\tau_2) \quad (3)$$

where K is constant and τ_2 describes inactivation. Curve-fitting was done with the standard Marquardt-Levenberg algorithm provided by Sigmaplot (Jandel, San Rafael, CA).

RESULTS

Fig. 1 shows whole-cell Ca^{2+} currents in nontransfected and transfected myotubes in response to 1-s depolarizing pulses from a holding potential of -40 mV . In nontransfected β -null cells, we observed a small sustained Ca^{2+} current previously identified as $I_{\beta\text{null}}$ (Beurg et al., 1997; Strube et al., 1998). $I_{\beta\text{null}}$ had a density considerably lower than the Ca^{2+} current density of normal myotubes and in many cells was entirely missing (9 of 38 cells). In β_{1a} -transfected (42 cells) and β_{2a} -transfected (52 cells) myotubes, we consistently observed large Ca^{2+} currents with densities typical of the normal L-type Ca^{2+} current (Table 1). In both types of transfected cells, Ca^{2+} currents activated at voltages more positive than -10 mV , had a slow activation, fast deactivation, and showed little inactivation except at large positive potentials. This Ca^{2+} current was previously identified in β_{1a} -transfected cells as the normal L-type Ca^{2+} current (Beurg et al., 1997). The present data show that a similar current was present in myotubes expressing β_{2a} . In separate experiments (not shown), we established that the β_{2a} -rescued Ca^{2+} current had the pharmacological profile of an L-type current by determining its increase or inhibition by the DHP agonist Bay K 8644 or antagonist nifedipine, respectively. When the holding potential was -80 mV , we

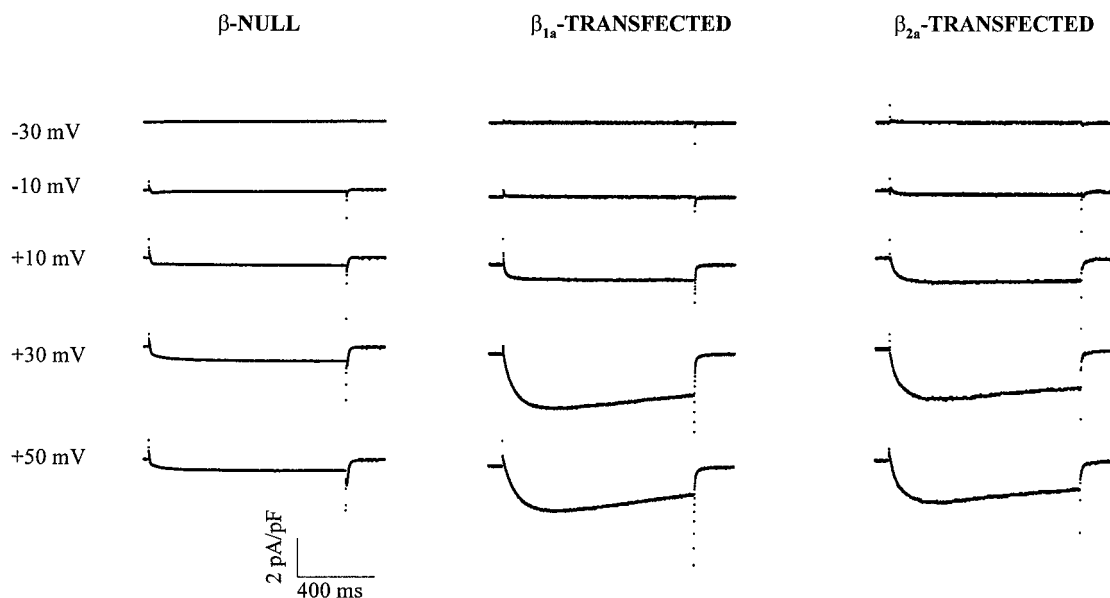


FIGURE 1 Ca^{2+} currents from a nontransfected (β -null) and transfected (β_{1a} or β_{2a}) myotubes in response to a 1-s depolarizing voltage step from a holding potential of -40 mV to the indicated potential. The charge carrier was $10 \text{ mM } \text{Ca}^{2+}$. Current and time scales are the same for all cells. Cell capacitances were 400, 330, and 220 pF, respectively.

TABLE 1 Average values of fitted parameters in normal, β_{1a} -transfected and β_{2a} -transfected myotubes

	<i>G-V</i> Curve			<i>Q-V</i> Curve			$\Delta F/F_0$ - <i>V</i> Curve		
	G_{\max} (pS/pF)	$V_{1/2}$ (mV)	k (mV)	Q_{\max} (nC/ μ F)	$V_{1/2}$ (mV)	k (mV)	$\Delta F/F_{0(\max)}$	$V_{1/2}$ (mV)	k (mV)
Normal									
Ca	168.4 \pm 9 (21)	12.2 \pm 0.7	5 \pm 0.3	6 \pm 0.5 (14)	12 \pm 4.3	14.3 \pm 0.8	2.7 \pm 0.2 (6)	1.4 \pm 2.4	8.9 \pm 1.3
Ba	164.1 \pm 12 (11)	4.6 \pm 2	4 \pm 0.4						
β_{1a} -transfected									
Ca	161.2 \pm 17 (9)	14.5 \pm 1.8	4.9 \pm 0.2	6.7 \pm 0.4 (8)	19 \pm 4.5	13 \pm 0.7	3.3 \pm 0.5 (9)	5 \pm 4.4	8.1 \pm 1.7
Ba	167.5 \pm 22 (7)	1.8 \pm 1.6	4.1 \pm 0.3						
β_{2a} -transfected									
Ca	152.7 \pm 5.2 (15)	10.4 \pm 0.8	5.2 \pm 0.3	2.7 \pm 0.2 (15)	12 \pm 2.8	14.3 \pm 1.1	1.1 \pm 0.2 (7)	0.6 \pm 3.5	5.6 \pm 1.7
Ba	157.7 \pm 25 (6)	-0.5 \pm 1.4	4.4 \pm 0.3						
β -null									
Ca	26.1 \pm 3 (38)	18.3 \pm 1.2	8.3 \pm 0.5	2.5 \pm 0.2 (12)	-6.1 \pm 3.8	12 \pm 1.6	—	—	—

All data (mean \pm SE) correspond to averages of Boltzmann parameters fitted of each cell. The number of myotubes is shown in parentheses. Measurements were done in 10 mM Ca^{2+} (Ca) or 10 mM Ba^{2+} (Ba).

observed a low-voltage-activated T-type Ca^{2+} current (not shown). Robust T-type Ca^{2+} currents were seen in $\sim 70\%$ of nontransfected and $\sim 30\%$ of transfected myotubes. We showed previously that the L-type Ca^{2+} current density of transfected myotubes remains unchanged up to day 16 of cell culture (Beurg et al., 1997). In the present study we collected and pooled data from transfected cells kept in culture for 8 to 12 days. In Table 1, the Ca^{2+} and Ba^{2+} conductances of transfected cells (G_{\max}) were compared to the density of the L-type conductance of normal myotubes kept in culture for a similar amount of time. According to an unpaired *t*-test, the difference between any two means (G_{\max}) had a *p* value ~ 0.2 , which made these data statistically indistinguishable. These results showed that expression of β_{2a} in β -null cells restored a Ca^{2+} current with a density typical of cells expressing β_{1a} and also of normal myotubes.

The voltage dependence of the Ca^{2+} and Ba^{2+} currents generated by transfection of β_{2a} were examined from the conductance-voltage (*G-V*) relationships. Conductances were computed by extrapolation of the maximal pulse currents to the reversal potential. Fig. 2 shows the normalized population average *G-V* curve of transfected and normal myotubes in 10 mM Ca^{2+} (filled symbols) or 10 mM Ba^{2+} (open symbols). The lines correspond to a Boltzmann fit to the population average. The fitted $G_{\text{Ca}}-V$ curve of β_{2a} -transfected cells was similar to that of normal and β_{1a} -transfected cells. The midpoints of these three curves were ~ 10 mV more positive than those fitted to the $G_{\text{Ba}}-V$ curves. Furthermore, all curves had a similar voltage dependence. Averages of Boltzmann parameters fitted to the *G-V* curves (Eq. 2) of each cell separately are shown in Table 1. From these results we concluded that the expression of the β_{2a} subunit in β -null cells was sufficient to restore an L-type Ca^{2+} current with a voltage dependence similar to that of β_{1a} -transfected cells or normal cells. Hence the Ca^{2+} current of cells transfected with β_{2a} were likely to originate from a complex of β_{2a} , α_{1S} , and possibly the other subunits of the skeletal DHPR complex.

We verified that the kinetics of activation of the L-type Ca^{2+} current in β_{2a} -transfected myotubes was similar to that of β_{1a} -transfected cells. The kinetics of activation of the skeletal L-type current is, to our knowledge, the slowest among all L-type Ca^{2+} currents. Expression studies in skeletal myotubes indicated that the kinetics of activation of Ca^{2+} channels with a cardiac-type α_{1C} pore subunit are severalfold faster than those with α_{1S} pore subunits (Tanabe

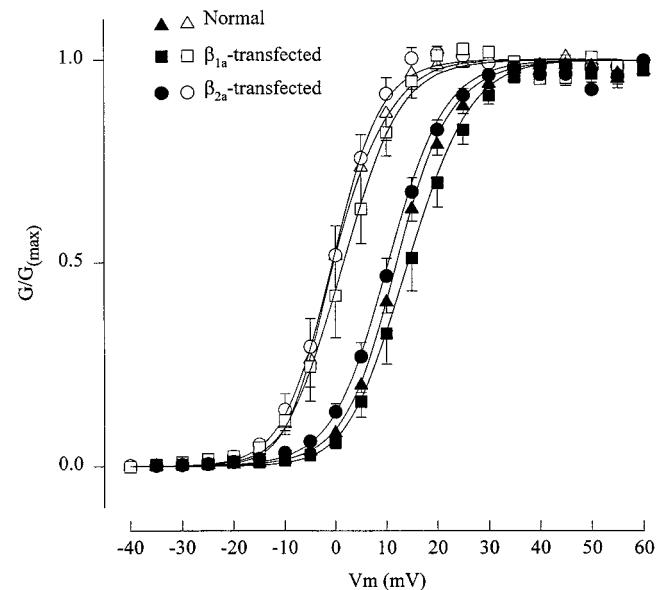


FIGURE 2 Voltage dependence of the average Ca^{2+} (filled symbols) or Ba^{2+} (open symbols) conductance in normal (21 cells for Ca^{2+} , 11 cells for Ba^{2+}), β_{1a} -transfected (9 cells for Ca^{2+} , 7 cells for Ba^{2+}) and β_{2a} -transfected myotubes (15 cells for Ca^{2+} , 6 cells for Ba^{2+}). Conductance was normalized according to the mean maximum conductance of each group of cells. Curves correspond to a Boltzmann fit of the population mean *G-V* curve. Parameters of the fit in Ca^{2+} were $V_{1/2} = 12.1$ mV, 14.5 mV, and 10.3 mV; $k = 5.3$ mV, 5.9 mV, and 5.6 mV for normal, β_{1a} -, and β_{2a} -transfected myotubes, respectively. Parameters of the fit in Ba^{2+} were $V_{1/2} = -0.2$ mV, 1.6 mV, and -0.7 mV; $k = 4.8$ mV, 5.4 mV, and 4.7 mV, respectively.

et al., 1991). Furthermore, the study above established that repeat I of the α_{1S} pore subunit was a molecular determinant of the slow kinetics of the skeletal L-type Ca^{2+} channel. Therefore, if the L-type Ca^{2+} current of β_{2a} -transfected myotubes originated from complexes that included α_{1S} and β_{2a} , these currents ought to display slow kinetics. Fig. 3 shows scaled traces of L-type current at +30 mV in β_{1a} - and β_{2a} -transfected myotubes. In these recording, we used a 1.5-s depolarizing pulse from a holding potential of -40 mV to fit both the activation and inactivation phases of the Ca^{2+} current. This was the longest pulse compatible with cell viability. The pulse current was fitted with Eq. 3, which conforms to a linear kinetic scheme with closed, open, and inactive states. A fit of $I(t)$ to the pulse current is shown by the curve superimposed on the current trace. In both types of transfected cells we found an excellent agreement between the fit and the pulse current. The plot in Fig. 3 shows the average time constant of activation, τ_1 in Eq. 3, for the indicated number of cells at positive potentials. Data are shown for normal and transfected myotubes. At each potential, the activation time constants fitted to each of the three myotube types were not significantly different according to an unpaired *t*-test. The fitted τ_1 agreed with previous determinations in normal myotubes (Beurg et al., 1997) and myotubes expressing chimeras of α_{1S} and α_{1C} when repeat I was from α_{1S} (Tanabe et al., 1991). All activation time constants in Fig. 3 were significantly higher than the 7-ms cutoff found for the kinetics of activation of chimeras carrying a repeat I of cardiac origin (Tanabe et al., 1991). Thus, the slow activation observed in cells transfected with β_{2a} suggests a direct interaction of this isoform with α_{1S} rather than other embryonic α_1 isoforms (see Discussion). We also compared the inactivation time constant, τ_2 in Eq. 3, in normal and transfected cells at a test potential of +20 mV. The inactivation time constants were 4.6 ± 1.5 s for normal (7 cells), 4.5 ± 1.3 s for β_{1a} -transfected (6 cells), and 3.8 ± 0.7 s for β_{2a} -transfected (13 cells) myotubes. However, the fitted inactivation time constant may not be entirely accurate because inactivation during the 1.5-s pulse was incom-

plete. In summary, the kinetics of the L-type current of myotubes expressing β_{2a} was indistinguishable from those of myotubes expressing β_{1a} and from normal myotubes. Consequently, the kinetics of Ca^{2+} channel activation in cells transfected with β_{2a} was deemed consistent with the presence of functional DHPR complexes that include α_{1S} and β_{2a} .

Even though the L-type current densities were the same, the density of functional Ca^{2+} channels and their maximum open probabilities may not be necessarily identical in myotubes expressing β_{2a} or β_{1a} . Consequently, we estimated these parameters using mean-variance analysis. Fig. 4, *A* and *B* show the time course of the mean Ca^{2+} current (*smooth trace*) and its intrinsic variance (*noisy trace*) following a pulse to +20 mV. Because Ca^{2+} currents were stable for no more than 40 or 50 pulses per cell, we further increased the signal-to-noise ratio of these determinations by averaging the ensemble variance and mean current over several cells after correction for cell capacitance. The mean currents and ensemble variances shown in Fig. 4 were averaged for nine cells expressing β_{2a} and for nine cells expressing β_{1a} . In both cell types, the superimposed traces of variance and mean current showed that the variance increased in proportion to the mean current throughout the pulse. Thus, the mean-variance relationships of β_{1a} - and β_{2a} -transfected myotubes displayed a comparatively small curvature, as shown in *C* and *D*. In these plots, $I\text{Ca}^{2+}$, the whole-cell Ca^{2+} current measured at the end of the pulse, averaged ~ 10 pA/pF and ~ 6 pA/pF, respectively, for the selected nine β_{1a} -transfected and nine β_{2a} -transfected cells. Since the variance increased in proportion to the current, the variance reached a higher value in the β_{1a} -transfected cells. The smooth line is a fit of the data according to Eq. 1 describing the relation between the mean current and its variance for channels with a single open conductance. Because the initial slope of the mean-variance curve was the same in the two cell types, the fitted single channel currents were approximately the same. In addition, the low level of curvature found in both plots implied that the density of

FIGURE 3 Kinetics of activation of the Ca^{2+} current of cells transfected with β_{1a} or β_{2a} . Traces were scaled to the maximum pulse current and are in response to a 1.5-s depolarizing voltage step from a holding potential of -40 mV to +30 mV. Curves superimposed on the trace correspond to a fit of the pulse current with Eq. 3 with parameters $K = -1.1$, $\tau_1 = 63$ ms, $\tau_2 = 4105$ ms for β_{1a} -, and $K = -1$, $\tau_1 = 72$ ms, $\tau_2 = 3956$ ms for β_{2a} -transfected myotubes. Graph shows the voltage dependence of the time constant of activation τ_1 (mean \pm SE) for the indicated number of cells.

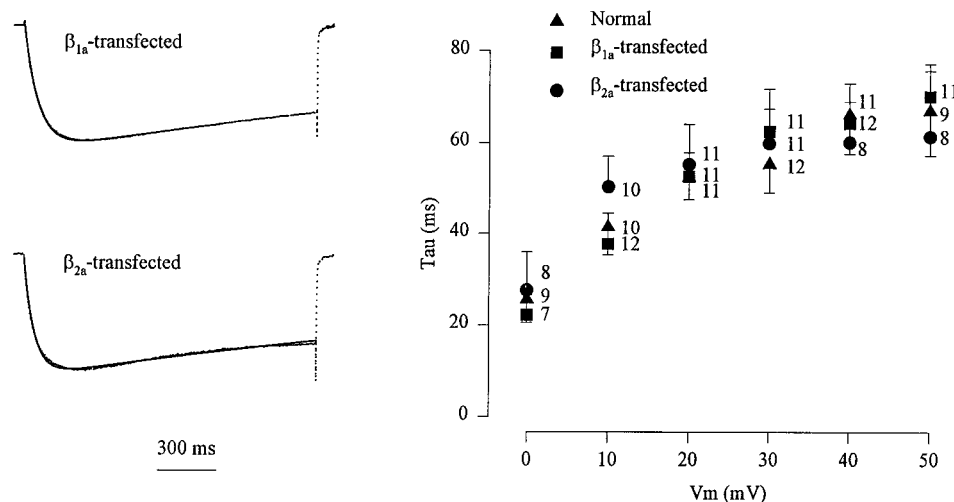
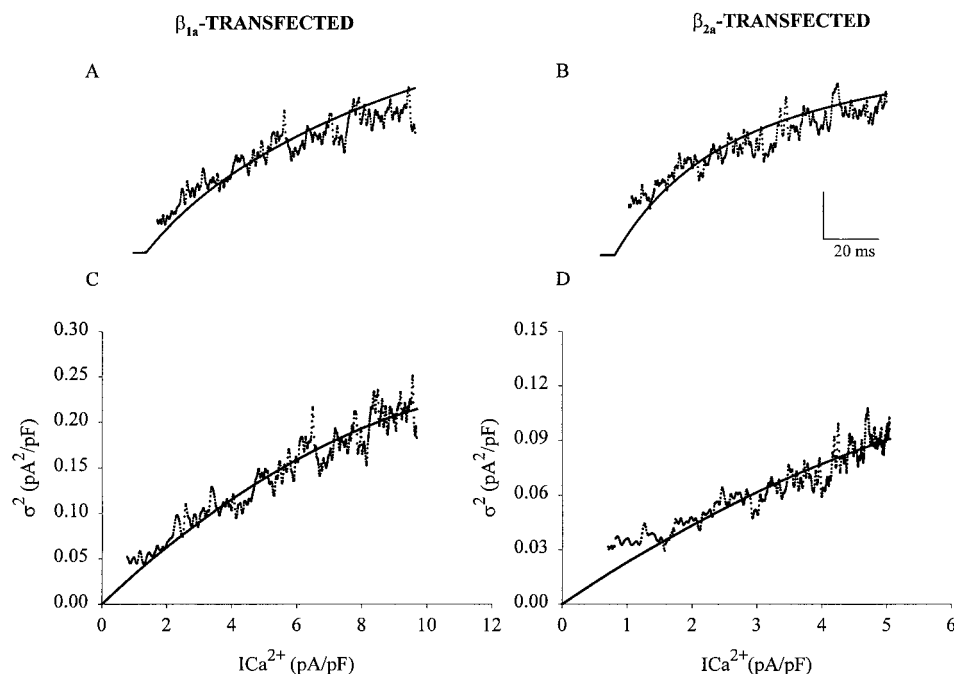


FIGURE 4 Mean-variance relationship of the L-type Ca^{2+} current of β_{1a} - and β_{2a} -transfected myotubes. Top traces show superimposed time courses of the whole-cell Ca^{2+} current (smooth trace) and the ensemble variance (noisy trace) for a step potential to +20 mV from a holding potential of -40 mV. Traces correspond to averages of nine cells transfected with β_{1a} and nine cells transfected with β_{2a} . Vertical calibration bar corresponds to $I_{\text{Ca}^{2+}} = 2.4$ pA/pF and $\sigma^2 = 0.05$ pA²/pF for β_{1a} - and $I_{\text{Ca}^{2+}} = 1.5$ pA/pF and $\sigma^2 = 0.028$ pA²/pF for β_{2a} -transfected myotubes. Bottom graphs show the ensemble variance plotted as function of the mean Ca^{2+} current for the same averages. Curves are a fit of the population mean-variance relationship with Eq. 1 with parameters $i = 0.034$ pA and $N_F = 843$ /pF for β_{1a} - and 0.024 pA and $N_F = 818$ /pF for β_{2a} -transfected cells.



Ca^{2+} channels was equally large in both cell types, and consequently the open probability at the time of maximal current ($I_{\text{Ca}^{2+}}^{\text{max}}/iN_F$) was equally low. The parameters of the parabolic fit of the population average variance-mean relationships are indicated in the figure legend and were consistent with previous determinations in normal myotubes (Strube et al., 1998; Beurg et al., 1998b). The population average p_{max} was somewhat higher than previously determined by cell-attached patch recordings, which in the presence of Bay K8644 was ~ 0.19 (Dirksen and Beam, 1995). A heterogeneous population of Ca^{2+} channels in which the majority of them have a low p_{max} and thus contribute little to the variance could explain this result (Strube et al., 1998). To provide for a statistical test of the data, we estimated i and N_F for each cell separately. In the nine cells of each group, N_F (mean \pm SE) was 970 ± 170 channels/pF and p_{max} was 0.31 ± 0.08 for β_{1a} -transfected cells, and N_F was 600 ± 115 channels/pF and p_{max} was 0.37 ± 0.07 for β_{2a} -transfected cells. In the nine cells of each group i was -42 ± 4 fA and -32 ± 3 fA, respectively. Neither N_F , p_{max} , nor i was significantly different according to an unpaired t -test. However, because the mean-variance curves were quasi-linear, N_F may represent a low-end estimate for this parameter and, therefore, p_{max} could be lower than estimated. However, i is determined by the initial slope of the mean-variance relationship, and therefore this parameter i is not affected by the degree of curvature of the mean-variance plot. In summary, the mean-variance analysis demonstrated that the permeation characteristics of the Ca^{2+} channels formed in myotubes expressing β_{1a} or β_{2a} were the same. Furthermore, the density of functional Ca^{2+} channels and their maximum open probability were not demonstrably different.

Next, we investigated whether the recovery of the L-type Ca^{2+} current in transfected myotubes occurred in parallel with a recovery of charge movements. Fig. 5 shows recordings of nonlinear capacitive currents in nontransfected and transfected myotubes. The pulse protocol included a 1-s depolarization to -20 mV to eliminate the immobilization-sensitive component of charge movements. The bulk of the remaining immobilization-resistant component is due to charge movements mediated by the DHPR (Strube et al., 1996). In β -null cells, the amplitude of the charge movement was severely reduced at all potentials, in agreement with previous results (Strube et al., 1996; Beurg et al., 1997). In β_{1a} -transfected cells, charge movements were significantly larger than in the nontransfected cells. The onset of ON and OFF components of charge movements occurred at ~ -20 mV and increased with voltage until a plateau was reached at potentials more positive than +40 mV. Quite surprisingly, the charge movements of β_{2a} -transfected cells were much smaller than those of β_{1a} -transfected cells. The peak amplitude of charge movements from β_{2a} -transfected cells were in most cases indistinguishable from those found in nontransfected cells. Charge movements were calculated for several cells by integration of the ON component on the nonlinear capacitance and the population averages were plotted as a function of voltage in Fig. 6 A. The Q_{max} of normal and β_{1a} -transfected myotubes was ~ 6.5 nC/ μF , in agreement with previous determinations (Beurg et al., 1997). This Q_{max} also agreed with determinations of others in normal and transfected α_{1S} -null dysgenic myotubes (Beam and Knudson, 1988; Garcia et al., 1994). The Q_{max} of nontransfected cells was ~ 2.7 -fold lower than that of normal and β_{1a} -transfected cells and, in addition, the $V_{1/2}$ of the Q - V curve of nontransfected cells was significantly

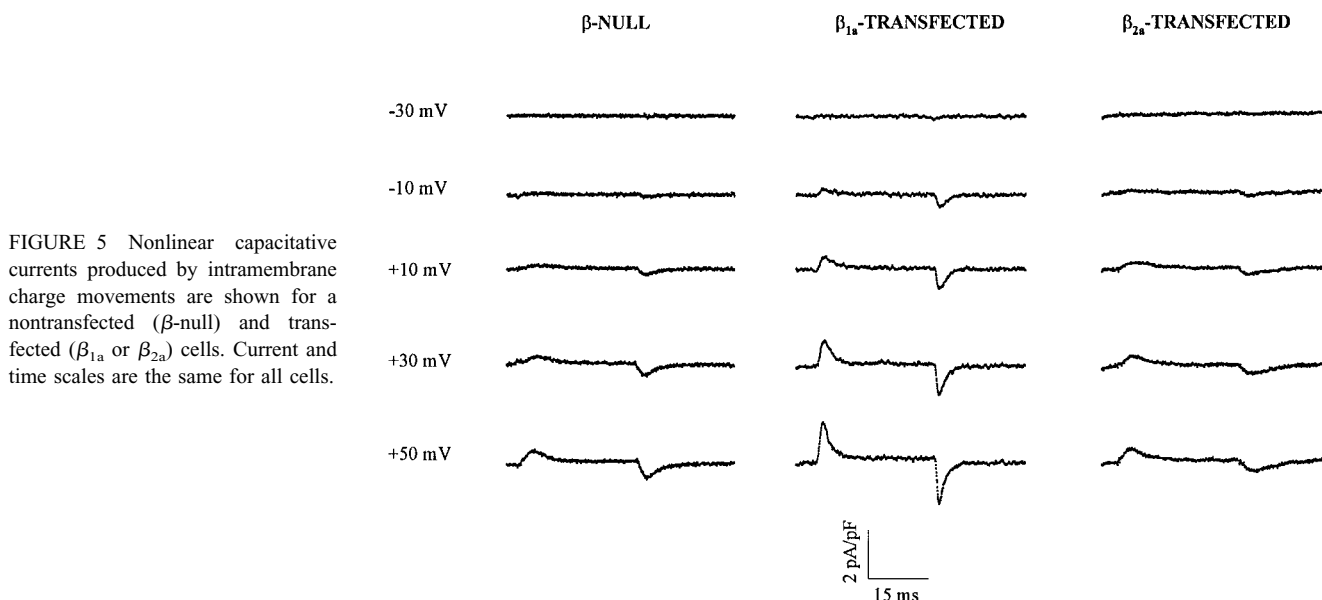


FIGURE 5 Nonlinear capacitive currents produced by intramembrane charge movements are shown for a nontransfected (β -null) and transfected (β_{1a} or β_{2a}) cells. Current and time scales are the same for all cells.

more negative. Both results agreed with previous determinations (Beurg et al., 1997). The Q_{\max} of β_{2a} -transfected cells was similar to that of nontransfected cells, a result that was entirely unexpected based on the density of the Ca^{2+} current of these cells. To compare the Q - V relationships of transfected cells, these data were normalized according to each Q_{\max} (Fig. 6 B). The Q - V curve of β_{2a} -transfected cells superimposes well with that of β_{1a} -transfected cells and both curves had a $V_{1/2}$ significantly more positive than that of nontransfected cells. Thus, the Q - V curve of β_{2a} -transfected cells had the Q_{\max} of nontransfected cells but the $V_{1/2}$ of β_{1a} -transfected cells. This observation suggested that the charge movements of β_{2a} cells were more likely to represent small charge movements of functional DHPRs rather than background charge movements of the β -null cell. Boltzmann parameters were fitted separately to each cell with Eq. 2 and these averages are shown in Table 1. A statistical analysis showed that the Q_{\max} of β_{1a} - and β_{2a} -transfected cells were significantly different (t -test, $p < 0.05$); however, the differences in $V_{1/2}$ were not ($p = 0.1$). We considered the possibility that charge movements in β_{2a} -transfected cells occurred at potentials more negative than the -80 mV holding potential. In this case, most of the charges would have already moved before the test pulse and the low Q_{\max} would reflect residual charges moved from -80 mV. We therefore delivered the same pulse protocol from -80 mV and from -120 mV to the same group of β_{2a} -transfected cells (Fig. 6 C). The inset shows that nonlinear capacitive currents at $+60$ mV delivered from either of the two holding potentials were indistinguishable. The bar histograms show the average Q_{\max} obtained from a fit of the Q - V curves at the two holding potentials. These values were 3.6 ± 0.4 and 3.3 ± 0.3 nC/ μF (4 cells) for HP -80 mV and -120 mV, respectively, and were statistically indistinguishable. In addition, Q_{\max} was measured by delivering the pulse protocol from HP -80 mV but delivering the reference

P/4 pulses from HP -120 mV. Again, we found that the Q_{\max} did not change (not shown). Finally, we performed charge movement protocols from HP -80 mV or HP -120 mV in normal and β_{1a} -transfected cells without a noticeable changes in Q_{\max} (not shown). These controls showed that charge movements in β_{2a} -transfected cells had an intrinsic low density. In conclusion, the β_{2a} subunit was a poor substitute for the β_{1a} subunit as a component of those DHPRs required for EC coupling.

To establish whether the measured charge movements in β_{2a} -transfected cells were significant for EC coupling, we investigated the recovery of intracellular Ca^{2+} transients. Because Ca^{2+} transients cannot be evoked by depolarization in nontransfected cells (Beurg et al., 1997), we could easily distinguish a fully recovered as well as a weakly recovered Ca^{2+} transient against the null background. Fig. 7 shows Ca^{2+} transients in a β_{1a} -transfected cell stimulated by a 50-ms test pulse from a holding potential of -40 mV. Measurements were made by confocal line-scans of fluo-3 fluorescence in voltage-clamped cells. Panel A shows line-scan images with time increasing from left to right and a vertical spatial dimension. The depolarizing pulse was delivered 100 ms after the start of the line scan, as indicated in the bottom of the figure. No effort was made to align cells relative to the scanning direction, as this was difficult to achieve. However, in most cases we scanned across the cell width rather than parallel to the long axis. The top and bottom edges of the line-scan images correspond to the top and bottom edges of the cell. Panel B shows traces of fluorescence averaged across the entire line-scan image. The time course of the Ca^{2+} current during the 50-ms pulse used to stimulate the Ca^{2+} transient is shown in panel C. Ca^{2+} transients were apparent at depolarizations more positive than -10 mV and in most cells produced a nonhomogeneous increase in cytosolic Ca^{2+} . The onset of the Ca^{2+} transient occurred simultaneously with the onset of the

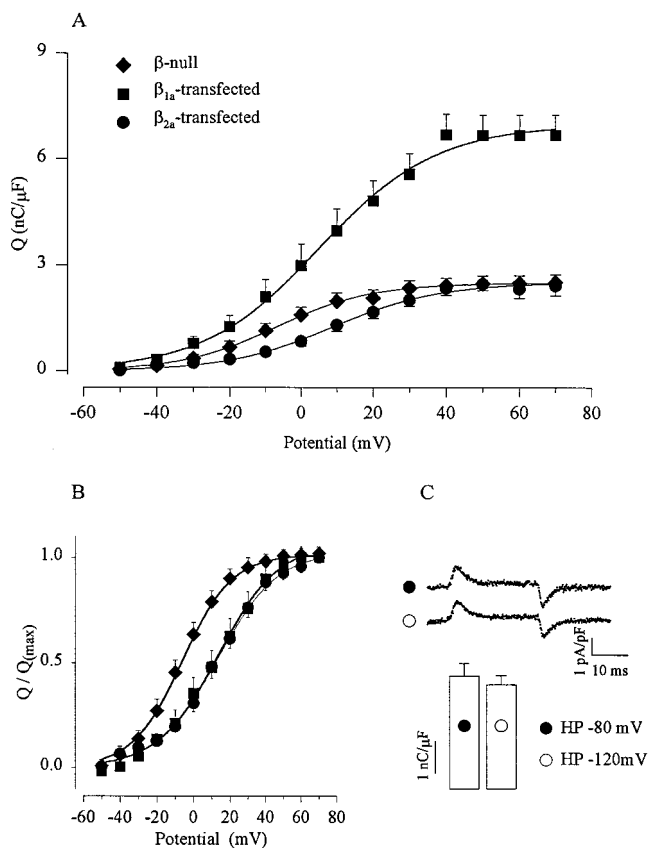


FIGURE 6 The voltage dependence of the intramembrane charge movements (mean \pm SE) are shown in (A) for β -null (12 cells), β_{1a} -transfected (8 cells), and β_{2a} -transfected (15 cells) myotubes. Curves correspond to a Boltzmann fit of the population mean Q - V curve. Parameters of the fit were $Q_{\max} = 2.5, 7,$ and 2.5 nC/ μ F; $V_{1/2} = -7, 5.5,$ and 8.8 mV; $k = 11.3, 16.3,$ and 14.6 mV, respectively. In (B), Q at each voltage was normalized according to the Q_{\max} of each group of cells. In (C), the histogram represents Q_{\max} (mean \pm SE) in the same β_{2a} -transfected myotubes (4 cells) recorded from a holding potential of -80 mV (filled symbols) and -120 mV (open symbols). Q_{\max} was 3.6 ± 0.4 and 3.3 ± 0.3 nC/ μ F, respectively, and was obtained from a Boltzmann fit of the Q - V curves. The recordings correspond to nonlinear capacitive currents in response to a test potential to $+60$ mV from a holding potential of -80 mV (upper trace) and -120 mV (lower trace) in the same β_{2a} -transfected myotube.

depolarization, and the time to maximum fluorescence was ~ 100 ms at all potentials. The amplitude of the transient increased with the amplitude of the pulse until a plateau was reached at potentials more positive than $+30$ mV. The decay phase of the transient outlasted the depolarization by a significant amount of time, in agreement with studies in normal rat and mouse myotubes in culture (Grouselle et al., 1991; Garcia and Beam, 1994). As shown in panel C, Ca^{2+} currents in the same cell declined in amplitude from $+30$ mV to $+70$ mV. However, no decline was observed in the amplitude of the Ca^{2+} transient at these potentials. Thus, Ca^{2+} transients in this range of potentials were independent of Ca^{2+} entry into the cell, consistent with previous results (Beurg et al., 1997).

Line-scan images of a Ca^{2+} transient in a β_{2a} -transfected cell are shown in Fig. 8. These Ca^{2+} transients were much

smaller than those of the β_{1a} -transfected cell. This is immediately obvious from the relative intensity of the images (A) and from the amplitude of the traces of integrated fluorescence as a function of time (B). Fig. 8 C shows the Ca^{2+} currents of the same β_{2a} -transfected cell during the period of stimulation of the Ca^{2+} transient. Comparison of panels B and C confirmed that Ca^{2+} transients in β_{2a} -transfected cells, like those in β_{1a} -transfected cells, were entirely controlled by voltage without participation of the Ca^{2+} current. The lack of participation of the Ca^{2+} current in triggering the Ca^{2+} transient was confirmed by recordings of Ca^{2+} transients in β_{2a} -transfected cells with Ca^{2+} currents blocked by $100 \mu\text{M}$ La^{3+} (not shown). We also plotted the amplitude of the Ca^{2+} transient as a function of the amplitude of the Ca^{2+} current in the same cell and found these to be entirely uncorrelated in either type of transfected cells ($r_{\text{corr}} < 0.5$; not shown). This was considered further evidence that Ca^{2+} entry into the cells played no role in the EC coupling of the transfected cells. Furthermore, the low amplitude of the transients of β_{2a} -transfected cells could not be explained by an impaired Ca^{2+} storage capacity since exposure of these cells to 5 mM caffeine resulted in a Ca^{2+} transient of normal amplitude (not shown). A comparison of Figs. 7 C and 8 C shows that the densities of Ca^{2+} currents in these two cells were similar. However, the maximum fluorescence intensity at maximal depolarization was ~ 3 -fold lower in the β_{2a} -transfected cell. At $+30$ mV, the mean (\pm SE) values of both parameters were $ICa^{2+} = -3.23 \pm 0.8$ pA and $\Delta F/F_0 = 1.04 \pm 0.16$ for β_{2a} -transfected cells (7 cells) and $ICa^{2+} = -3.25 \pm 0.44$ pA and $\Delta F/F_0 = 3.2 \pm 0.44$ for β_{1a} -transfected cells (8 cells). This difference in evoked fluorescence was statistically significant (t -test, $p < 0.05$). In summary, a skeletal-type EC coupling was restored in myotubes expressing β_{2a} . However, the Ca^{2+} transients of these myotubes were small despite the presence of Ca^{2+} currents with a normal density. This result strongly suggested that the lack of complete recovery of EC coupling was not due to an overall low level of β_{2a} expression in the β -null myotube.

The voltage dependence of the Ca^{2+} transients of transfected cells were investigated to determine which parameters were modified by expression of β_{2a} . Fig. 9 shows $\Delta F/F_0$ at the peak of the transient as a function of voltage. The lines correspond to a fit of the population average $\Delta F/F_0$ - V curve with a Boltzmann equation (Eq. 2). In both cell types, $\Delta F/F_0$ increased in a sigmoidal manner, reaching a maximum for depolarizations more positive than $+30$ mV. In β_{1a} -transfected cells, $\Delta F/F_{0(\max)}$ was significantly higher than in β_{2a} -transfected cells, and the difference was statistically significant (nonpaired t -test $p < 0.05$). In β_{1a} - (9 cells) and β_{2a} -transfected (8 cells) myotubes the highest and lowest $\Delta F/F_{0(\max)}$ were $5.5/2.0$ and $1.6/0.4$, respectively. Averages of Boltzmann parameters fitted separately to each cell are shown in Table 1. Parameters k and $V_{1/2}$ are in agreement with previous studies in normal myotubes, β_{1a} -rescued β -null myotubes, and α_{1S} -rescued dysgenic myotubes (Garcia and Beam, 1994; Beurg et al., 1997).

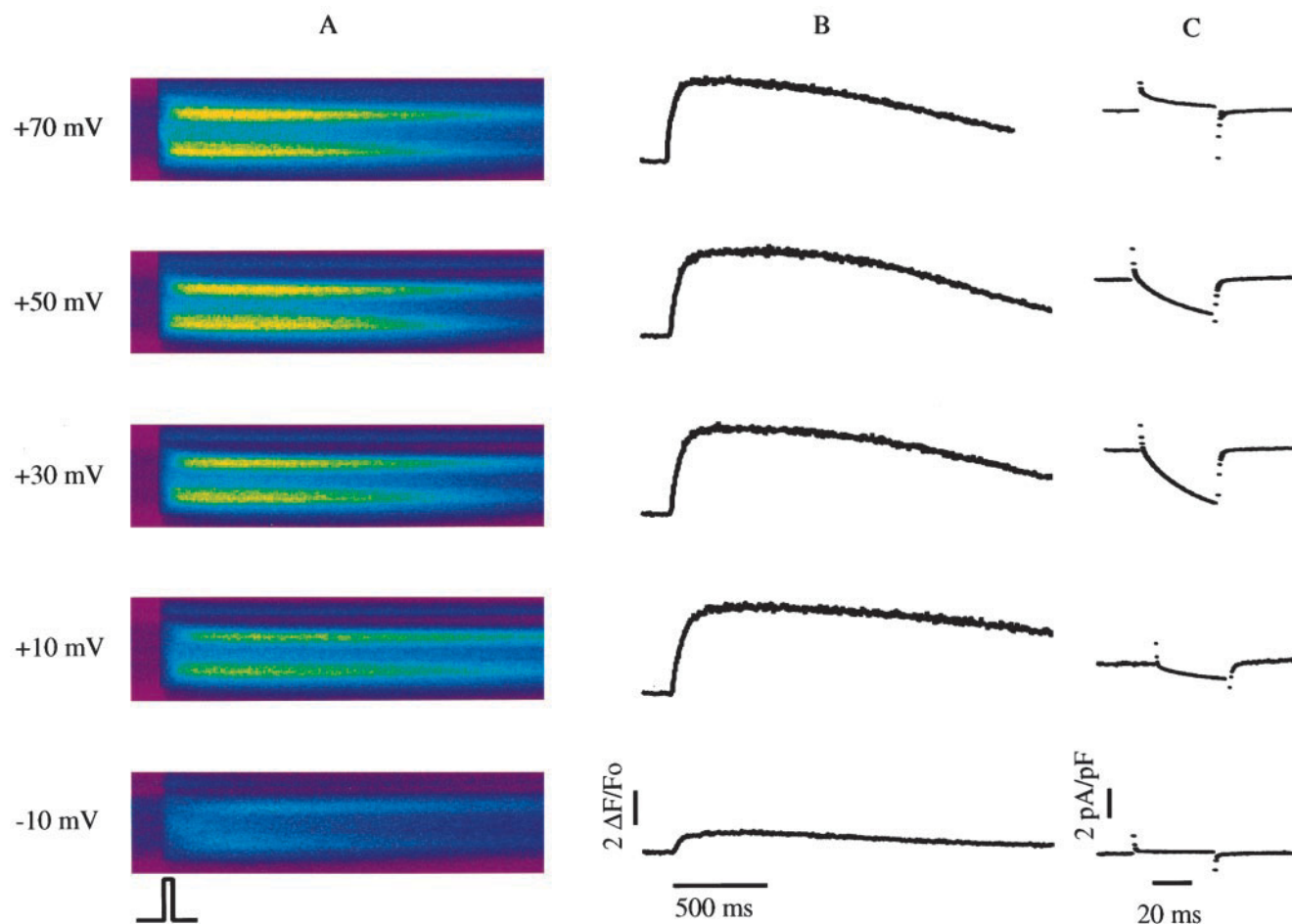


FIGURE 7 Intracellular Ca^{2+} transients under whole-cell clamp in a β_{1a} -transfected myotube. (A) Confocal line-scan images of fluo-3 fluorescence at the indicated pulse potentials from a holding potential of -40 mV. The spatial dimension is vertical and the temporal dimension is horizontal. The pulse potential duration was 50 ms and was delivered 120 ms after the initiation of the line-scan as indicated in the bottom. Images have a dimension of $47.5 \mu\text{m}$ (vertical) and 2.05 s (horizontal) and a pixel size of $0.25 \mu\text{m} \times 2.05 \text{ ms}$. Each image is from the same line location in the myotube. (B) Time course of fluorescence intensity in $\Delta F/F_0$ units obtained by integration of the image fluorescence. (C) Ca^{2+} currents elicited by the pulse potential in the same cell.

However, $\Delta F/F_0$ was much higher than in these previous nonconfocal determinations. These results demonstrated that a complex of α_{1S} and β_{2a} could not fully restore skeletal-type EC coupling. In addition, the restored EC coupling was insufficient to restore cell contraction. However, a cell contraction could be evoked by caffeine (not shown).

DISCUSSION

The Ca^{2+} current density, its voltage dependence, kinetics of activation, and estimated single channel currents were indistinguishable in β -null myotubes expressing β_{1a} or β_{2a} . This identity suggests that both subunits became integrated into functional skeletal-type DHPR complexes formed by α_{1S} , β_{1a} or β_{2a} , and presumably $\alpha_2\text{-}\delta$ and γ subunits. This conclusion also accounts for the fact that both the homologous complex containing β_{1a} and the heterologous complex containing β_{2a} participated in the expression of skeletal-

type EC coupling, which requires a skeletal-type α_{1S} pore subunit. The $\alpha_2\text{-}\delta$ and γ subunits may also have formed part of the expressed DHPR complex, since L-type Ca^{2+} currents of normal density and kinetics require $\alpha_2\text{-}\delta$ and γ (Wei et al., 1991; Felix et al., 1997). Critical differences between the expression of β_{1a} and β_{2a} in β -null cells were observed in the density of charge movements and the amplitude of the Ca^{2+} transients. In cells expressing β_{2a} , the maximal density of the charge movements was ~ 2.5 times lower and the amplitude of the Ca^{2+} transients was 3 to 5 times lower than those observed in cells expressing β_{1a} . From these last two results it can be concluded that β_{2a} was incapable of entirely substituting for β_{1a} in those DHPRs required for EC coupling.

To understand how Ca^{2+} currents and EC coupling are regulated by β , it is essential that we dismiss possible interactions between the expressed β isoforms and non- α_{1S} isoforms. Embryonic myotubes express a minor amount of an unidentified α_1 isoform, $\alpha_{1\text{dys}}$, different from α_{1S} and

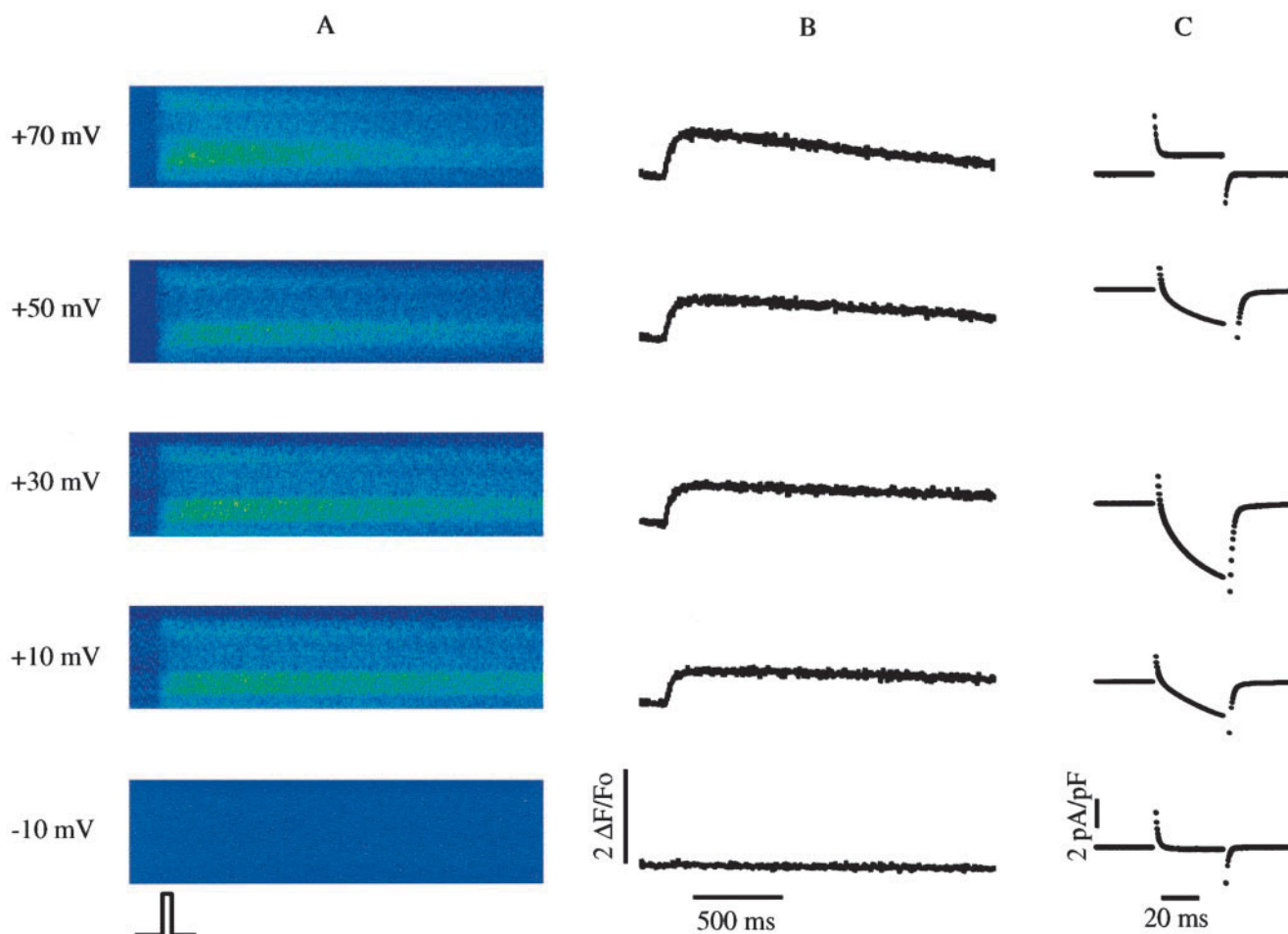


FIGURE 8 Intracellular Ca^{2+} transients under whole-cell clamp in a β_{2a} -transfected myotube. (A) Confocal line-scan images of fluo-3 fluorescence at the indicated pulse potentials of 50 ms from a holding potential of -40 mV. Images have a dimension of $25 \mu m$ (vertical) and 2.05 s (horizontal). (B) Time course of fluorescence intensity in $\Delta F/F_o$ units obtained by integration of the image fluorescence. (C) Ca^{2+} currents elicited by the pulse potential in the same cell.

presumed to be an embryonic homolog of α_{1C} (Chaudhari and Beam, 1993). Expression of this isoform accounts for the presence in β -null cells of I_{dys} , a low-density background Ca^{2+} current initially identified in α_{1S} -deficient dysgenic myotubes (Adams and Beam, 1989; Strube et al., 1998). In principle, β_{2a} or β_{1a} could have formed a complex with α_{1dys} instead of a complex with α_{1S} . Such α_{1dys}/β complexes, if present, should contribute to the L-type Ca^{2+} current density since β_{1a} or β_{2a} are known to increase the density of Ca^{2+} currents when coexpressed with α_{1C} in a mammalian cell line (Chien et al., 1995; Kamp et al., 1996). We believe these putative α_{1dys}/β_{1a} or α_{1dys}/β_{2a} channels were not formed in β -null myotubes. First, the I_{dys} Ca^{2+} channels have an estimated single channel current that is much larger than those underlying the β_{1a} - or β_{2a} -rescued Ca^{2+} currents (-84 ± 9 fA for I_{dys} , Strube et al., 1998; vs. -42 ± 4 fA for β_{1a} currents and -32 ± 3 fA for β_{2a} currents all at $+20$ mV in 10 mM external Ca^{2+}). Second, we transfected dysgenic myotubes that lack a functional α_{1S} with either β_{1a} or β_{2a} plus CD8 as marker. None of the dysgenic myotubes expressing CD8 displayed slow high-

density skeletal-type Ca^{2+} currents. Finally, we expressed β_{1a} , β_{2a} , and α_{1S} separately from each other in double mutant α_{1S} -deficient β_1 -deficient myotubes produced by breeding heterozygous $\alpha_{1S}(\pm)$ and $\beta_1(\pm)$ mice (Ahern et al., 1999). Single α_{1S} or β subunits rescued Ca^{2+} currents with a maximum density <0.2 pA/pF in the double mutant expression system. All these controls convinced us that the recovered L-type Ca^{2+} current originated exclusively from complexes of α_{1S} and the overexpressed β isoform. The lack of a significant contamination by α_{1dys}/β channels was presumably due to the low level of expression of this particular α_1 isoform in β -null myotubes.

It is reasonable to assume that DHPRs that include β_{1a} accumulated at a higher density in the cell surface than DHPRs with β_{2a} . This is based entirely in the difference in Q_{max} and takes into consideration the fact that ensemble noise and gating current measurements done by others have shown that β_{1a} and β_{2a} do not alter the intrinsic number of gating charges of the Ca^{2+} channel (Neely et al., 1993; Kamp et al., 1996; Noceti et al., 1996). However, those additional DHPRs expressed in β_{1a} -transfected cells did not

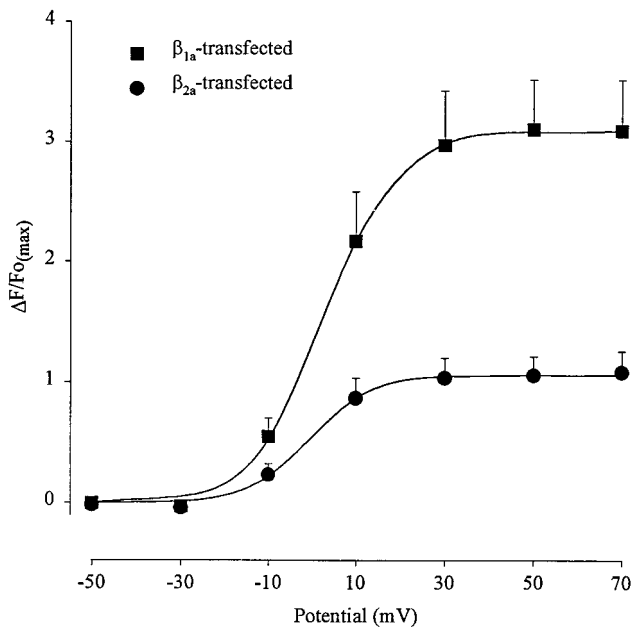


FIGURE 9 Voltage dependence of Ca^{2+} transients in transfected myotubes. Ca^{2+} transients were elicited in β_{1a} - ($n = 9$ cells) and β_{2a} - ($n = 7$ cells) transfected myotubes by voltage steps of 50 ms from a holding potential of -40 mV. $\Delta F/Fo$ at the peak of the transient (mean \pm SE) was obtained by integration of confocal line-scan images. Curves correspond to a Boltzmann fit of the population mean $\Delta F/Fo_{(max)}-V$ curve. Parameters of the fit were $\Delta F/Fo_{(max)} = 3.1$ and 1.1 ; $V_{1/2} = 3$ and -0.6 mV; $k = 8.2$ and 7.1 mV, respectively.

contribute equally to the macroscopic Ca^{2+} current and charge movements. If this were the case, the open probability or the unitary conductance of Ca^{2+} channels produced by α_{1S}/β_{1a} complexes should have been significantly lower than that produced by α_{1S}/β_{2a} complexes. This conclusion is forced by the similarity in macroscopic L-type Ca^{2+} current densities between the two transfected cell types. The ensemble noise measurements do not support this view. Variance analysis showed that $i(+20$ mV) was the same for both cell types, a result consistent with measurements showing that β isoforms do not alter the single channel conductance (Bourinet et al., 1996). Furthermore, since the degree of curvature of the variance-mean plots was equally low (Fig. 4), the p_{max} must also be equally low. Based on these considerations, it is likely that those additional DHPRs expressed in β_{1a} -transfected cells contributed far less to the Ca^{2+} current than to charge movements. This conclusion is consistent with measurements of Ca^{2+} channel density and charge movements produced by the α_{1E}/β_{1a} and α_{1E}/β_{2a} isoform pairs. These measurements indicate that a set of gating charges in Ca^{2+} channels with β_{1a} produced gating currents that did not contribute to the opening of the channel (Noceti et al., 1996). Thus, the β_{1a} isoform may be intrinsically prone to produce uncoupling of charge movements in the α_{1S} subunit from the opening of the Ca^{2+} channel. Uncoupling of these two events could be a key step in the recruitment of DHPRs for triggering EC coupling.

The sequential steps by which α_{1S}/β_{1a} complexes become coupled to RyRs and to SR Ca^{2+} release remain speculative at this point. The same can be said of those events that may have prevented expression of charge movements in complexes of α_{1S} and β_{2a} . DHPR β_{2a} subunits have been shown to be critically involved in increasing the cell surface expression of α_{1C} subunits (Chien et al., 1995). Furthermore, different DHPR β isoforms are found in a complex with α_1 isoforms in different cellular compartments. In the heterologous tsA201 expression system α_{1S}/β_{1a} complexes are predominantly found in the endoplasmic reticulum, whereas α_{1S}/β_{2a} complexes are associated with the plasma membrane (Neuhuber et al., 1998). Thus, it could be argued that a β subunit-specific event directed α_{1S}/β_{1a} complexes to the T-tubule/SR junctional domains involved in EC coupling, whereas α_{1S}/β_{2a} were directed away from T-tubule/SR junctions. This could explain the fact that EC coupling was only partially restored by the combined expression of α_{1S} and β_{2a} . We do not believe that a mistargeting of DHPRs accounts for the incomplete EC coupling in this case. Recent observations suggest that functional expression of Ca^{2+} channels requires interactions between DHPRs and RyRs. Nakai et al. (1996) showed in myotubes specifically lacking ryanodine receptors (RyR-1), that Ca^{2+} currents are significantly reduced despite the presence of charge movements with an almost normal density. Thus, interactions of DHPRs and RyRs may be required for the expression of the normal L-type Ca^{2+} currents. A domain in RyR-1 was shown to be essential for a retrograde signal that stabilizes the DHPR Ca^{2+} current (Nakai et al., 1998). Because cells expressing β_{1a} and β_{2a} had identical L-type Ca^{2+} currents it can be inferred that DHPRs that include β_{1a} or β_{2a} were equally capable of functional interactions with RyRs. Consequently, targeting events critical for the surface location of voltage sensors and RyRs but occurring before the establishment of functional interactions between these two receptors are unlikely to explain the phenotype of cells expressing β_{2a} .

Because β_{2a} -transfected cells expressed a normal L-type Ca^{2+} current, but in these cells EC coupling was minimal, we suggest that these two inherent functions of the skeletal-type DHPR are controlled by different domains of the β subunit. For example, a domain common to β_{1a} and β_{2a} may be sufficient for expression of the L-type Ca^{2+} current, while a β_{1a} -specific domain may enhance or a β_{2a} -specific domain may attenuate expression of charge movements required for EC coupling. Amino acid sequence comparison between the β_{1a} and β_{2a} isoforms reveals two central regions that are conserved among all β isoforms, a nonconserved linker region between the two conserved domains and distinct N-terminal and C-terminal domains (Perez-Reyes and Schneider, 1994). In addition, a ~ 20 amino acid region of interaction with α_{1S} is present in all isoforms (De Waard et al., 1994). Major differences between β_{2a} and β_{1a} are found in the C-terminal region which in β_{2a} is ~ 115 amino acids longer. The C-terminal region of β_{2a} is predicted as highly hydrophilic and flexible; hence it may

represent an appropriate surface for interactions with cytoplasmic proteins including secondary interactions with the cytoplasmic loops of the α_{1S} subunit. Such interaction could conceivably disrupt the normal function of those DHPRs triggering EC coupling. Recent data suggest that deletion of the C-terminal region of β_{2a} increases EC coupling, whereas deletion of the C-terminal region of β_{1a} decreases EC coupling, but has a minor effect on charge movements (Beurg et al., 1999). Expression of chimeras and deletion mutants of β_{1a} and β_{2a} in β -null myotubes should serve to establish the structural determinants of the DHPR β subunit required for expression of Ca^{2+} currents and EC coupling.

This work was supported by National Institutes of Health Grant HL-47053 (to R.C., P.A.P., and R.G.G.), National Science Foundation Grant IBN-93/9340 (to R.G.G. and P.A.P.), and a grant from the Wisconsin Heart Association (to M.B. and M.W.C.).

REFERENCES

- Adams, B. A., and K. G. Beam. 1989. A novel calcium current in dysgenic skeletal muscle. *J. Gen. Physiol.* 94:429–444.
- Ahern, C. A., P. Powers, R. Gregg, and R. Coronado. 1999. Expression of cardiac DHPR α_{1C} in α_{1I}/β_{1I} -double mutant skeletal muscle myotubes. *Biophys. J.* 76:467a(abstr.).
- Beam, K. G., and C. M. Knudson. 1988. Calcium current in embryonic and neonatal mammalian skeletal muscle. *J. Gen. Physiol.* 91:781–798.
- Beurg, M., C. A. Ahern, P. Powers, R. G. Gregg, and R. Coronado. 1999. Domain of calcium channel β subunit involved in excitation contraction coupling. *Biophys. J.* 76:394a(abstr.).
- Beurg, M., C. Ahern, and R. Coronado. 1998b. Low open probability skeletal L-type calcium channel revealed by ensemble variance analysis. *Biophys. J.* 74:164a. (Abstr.).
- Beurg, M., C. Ahern, M. Sukhareva, E. Perez-Reyes, P. Powers, R. Gregg, and R. Coronado. 1998a. The dihydropyridine receptor β_1 subunit is specifically required for excitation-contraction coupling of skeletal muscle. *Biophys. J.* 74:235a. (Abstr.).
- Beurg, M., M. Sukhareva, C. Strube, P. A. Powers, R. G. Gregg, and R. Coronado. 1997. Recovery of Ca^{2+} current, charge movements, and Ca^{2+} transients in myotubes deficient in dihydropyridine receptor β_1 subunit transfected with β_1 cDNA. *Biophys. J.* 73:807–818.
- Bourinet, E., G. W. Zamponi, A. Stea, T. W. Soong, B. A. Lewis, L. P. Jones, D. T. Yue, and T. P. Snutch. 1996. The α_{1E} calcium channel exhibits permeation properties similar to low-voltage-activated calcium channels. *J. Neurosci.* 16:4983–4993.
- Castellano, A., X. Wei, L. Birnbaumer, and E. Perez-Reyes. 1993. Cloning and expression of a neuronal calcium channel β subunit. *J. Biol. Chem.* 268:12359–12366.
- Chaudhari, N., and K. G. Beam. 1993. mRNA for cardiac calcium channel is expressed during development of skeletal muscle. *Dev. Biol.* 155:507–515.
- Chien, A. J., X. L. Zhao, R. E. Shirokov, T. S. Puri, C. F. Chang, D. Sun, E. Rios, and M. M. Hosey. 1995. Roles of a membrane-localized beta subunit in the formation and targeting of functional L-type Ca^{2+} channels. *J. Biol. Chem.* 270:30036–30044.
- Conklin, M., P. Powers, R. G. Gregg, and R. Coronado. 1998. Ca^{2+} sparks in embryonic mouse skeletal muscle selectively deficient in dihydropyridine receptor α_{1S} or β_1 subunits. *Biophys. J.* (in press).
- De Waard, M., M. Pragnell, and P. K. Campbell. 1994. Ca^{2+} channel regulation by a conserved β subunit domain. *Neuron.* 13:495–503.
- Dirksen, R. T., and K. G. Beam. 1995. Single calcium channel behavior in native skeletal muscle. *J. Gen. Physiol.* 105:227–247.
- Felix, R., C. A. Gurnett, M. De Waard, and P. K. Campbell. 1997. Dissection of functional domains of the voltage-dependent Ca^{2+} channel $\alpha_{2\delta}$ subunit. *J. Neurosci.* 17:6884–6891.
- Garcia, J., and K. G. Beam. 1994. Measurement of calcium transients and slow calcium current in myotubes. *J. Gen. Physiol.* 103:107–123.
- Garcia, J., T. Tanabe, and K. G. Beam. 1994. Relationship of calcium transients to calcium currents and charge movements in myotubes expressing skeletal and cardiac dihydropyridine receptors. *J. Gen. Physiol.* 103:125–147.
- Gregg, R. G., A. Messing, C. Strube, M. Beurg, R. Moss, M. Behan, M. Sukhareva, S. Haynes, J. A. Powell, R. Coronado, and P. Powers. 1996. Absence of the β subunit (*cchb1*) of the skeletal muscle dihydropyridine receptor alters expression of the α_1 subunit and eliminates excitation-contraction coupling. *Proc. Natl. Acad. Sci. USA.* 93:13961–13966.
- Grouselle, M., J. Koenig, M. L. Lascombe, J. Chapron, P. Meleard, and D. Georgescauld. 1991. Fura-2 imaging of spontaneous and electrical oscillations of intracellular free Ca^{2+} in rat myotubes. *Pflügers Arch.* 418:40–50.
- Heinemann, S. H., and F. Conti. 1992. Nonstationary analysis and application to patch clamp recordings. In *Ion channels*. B. Rudy and L. E. Iverson, editors. Methods in Enzymology. Vol. 207 Book series. Academic Press, San Diego, CA. 131–148.
- Hullin, R., D. Singer-Lahat, M. Freichel, M. Biel, N. Dascal, F. Hofmann, and V. Flockerzi. 1992. Calcium channel beta subunit heterogeneity: functional expression of cloned cDNA from heart, aorta and brain. *EMBO J.* 11:885–890.
- Josephson, I. R., and G. Varadi. 1996. The β subunit increases Ca^{2+} currents and gating charge movements of human cardiac L-type Ca^{2+} channels. *Biophys. J.* 70:1285–1293.
- Kamp, T., M. T. Perez-Garcia, and E. Marban. 1996. Enhancement of ionic current and charge movement by coexpression of calcium channel β_{1a} subunit with α_{1C} subunit in a human embryonic kidney cell line. *J. Physiol.* 492:89–96.
- Lacerda, A. E., H. S. Kim, P. Ruth, E. Perez-Reyes, and V. Flockerzi. 1991. Normalization of current kinetics by interaction between the α_1 and β subunits of the skeletal muscle dihydropyridine-sensitive Ca^{2+} channel. *Nature.* 352:527–530.
- Lamb, G. D. 1992. DHP receptor and excitation-contraction coupling. *J. Muscle Cell Motil.* 13:394–405.
- Lory, P., G. Varadi, and A. Schwartz. 1992. The β subunit controls the gating and the dihydropyridine sensitivity of the skeletal muscle Ca^{2+} channel. *Biophys. J.* 63:1421–1424.
- Nakai, J., R. T. Dirksen, H. T. Nguyen, I. N. Pessah, K. G. Beam, and P. D. Allen. 1996. Enhanced dihydropyridine channel activity in the presence of ryanodine receptor. *Nature.* 380:72–75.
- Nakai, J., N. Sekiguchi, T. A. Rando, P. D. Allen, and K. G. Beam. 1998. Two regions of the ryanodine receptor involved in coupling with L-type Ca^{2+} channels. *J. Biol. Chem.* 273:13403–13406.
- Neely, A., X. Wei, R. Olcese, L. Birnbaumer, and E. Stefani. 1993. Potentiation by the β subunit of the ratio of the ionic current to the charge movement in the cardiac calcium channel. *Science.* 262:575–578.
- Neuhuber, B., U. Gerster, J. Mitterdorfer, H. Glossmann, and B. E. Flucher. 1998. Differential effects of Ca^{2+} channel β_{1a} and β_{2a} subunits on complex formation with α_{1S} and on current expression in tsA201 cells. *J. Biol. Chem.* 273:9110–9118.
- Nishimura, S., H. Takeshima, F. Hofmann, V. Flockerzi, and K. Imoto. 1993. Requirement of the calcium channel β subunit for functional conformation. *FEBS Lett.* 324:283–286.
- Noceti, F., P. Baldelli, X. Wei, N. Qin, L. Toro, L. Birnbaumer, and E. Stefani. 1996. Effective gating charges per channel in voltage-dependent K^{+} and Ca^{2+} channels. *J. Gen. Physiol.* 108:143–155.
- Olcese, R., A. Neely, N. Qin, X. Wei, L. Birnbaumer, and E. Stefani. 1996. Coupling between charge movement and pore opening in vertebrate neuronal α_{1E} calcium channels. *J. Physiol.* 497:3:675–686.
- Olcese, R., N. Qin, T. Schneider, A. Neely, X. Wei, E. Stefani, and L. Birnbaumer. 1994. The amino terminus of a calcium channel β subunit sets rates of channel inactivation independently of the subunit's effect on activation. *Neuron.* 13:1433–1438.
- Perez-Garcia, M. T., T. J. Kamp, and E. Marban. 1995. Functional properties of cardiac L-type calcium channels transiently expressed in HEK293 cells. Role of alpha1 and beta subunits. *J. Gen. Physiol.* 105:289–306.
- Perez-Reyes, E., A. Castellano, H. S. Kim, P. Bertrand, E. Bagstrom, A. Lacerda, X. Wei, and L. Birnbaumer. 1992. Cloning and expression of

- a cardiac/brain β subunit of the L-type calcium channel. *J. Biol. Chem.* 267:1792–1797.
- Perez-Reyes, E., and T. Schneider. 1994. Calcium channels: structure, function, and classification. *Drug Dev. Res.* 33:295–318.
- Pizarro, G., G. Brum, M. Fill, R. Fitts, M. Rodriguez, I. Uribe, and E. Rios. 1988. The voltage sensor of excitation-contraction coupling: a comparison with Ca^{2+} channels. In *The Calcium Channel, Structure, Function, and Implications*. M. Morad, W. Nayler, S. Kazda, and M. Schramm, editors. Springer Verlag, Berlin. 138–158.
- Powers, P. A., S. Liu, K. Hogan, and R. G. Gregg. 1992. Skeletal muscle and brain isoforms of a β subunit of human voltage-dependent calcium channels are encoded by a single gene. *J. Biol. Chem.* 267:22967–22972.
- Pragnell, M., M. De Waard, Y. Mori, T. Tanabe, T. P. Snutch, and K. P. Campbell. 1994. Calcium channel β -subunit binds to a conserved motif in the I-II cytoplasmic linker of the α_1 -subunit. *Nature*. 368:67–70.
- Quin, N., R. Olcese, J. Zhou, O. A. Cabello, L. Birnbaumer, and E. Stefani. 1996. Identification of a second region of the β -subunit involved in regulation of calcium channel inactivation. *Am. J. Physiol.* 271: C1539–C1545.
- Ruth, P., A. Rohrkasten, M. Biel, E. Bosse, S. Regulla, H. E. Meyer, V. Flockerzi, and F. Hofmann. 1989. Primary structure of the β subunit of the DHP-sensitive calcium channel from skeletal muscle. *Science*. 245: 1115–1118.
- Singer, D., M. Biel, I. Lotan, V. Flockerzi, F. Hofmann, and N. Dascal. 1991. The role of the subunits in the function of calcium channel. *Science*. 253:1553–1557.
- Stea, A., S. J. Dubel, M. Pragnell, J. P. Leonard, K. P. Campbell, and T. P. Snutch. 1993. A β subunit normalizes the electrophysiological properties of a cloned N-type Ca^{2+} channel $\alpha 1$ subunit. *Neuropharmacology*. 32:1103–1116.
- Strube, C., M. Beurg, P. A. Powers, R. G. Gregg, and R. Coronado. 1996. Reduced Ca^{2+} current, charge movement, and absence of Ca^{2+} transients in skeletal muscle deficient in dihydropyridine receptor β_1 subunit. *Biophys. J.* 71:2531–2543.
- Strube, C., M. Beurg, C. Sukhareva, J. A. Ahern, C. Powell, P. A. Powers, R. G. Gregg, and R. Coronado. 1998. Molecular origin of the Ca^{2+} current of skeletal muscle myotubes selectively deficient in dihydropyridine receptor β_1 subunit. *Biophys. J.* 75:207–217.
- Tanabe, T., B. A. Adams, S. Numa, and K. G. Beam. 1991. Repeat I of the dihydropyridine receptor is critical in determining calcium channel activation kinetics. *Nature*. 352:800–803.
- Tanabe, T., K. G. Beam, J. A. Powell, and S. Numa. 1988. Restoration of excitation-contraction coupling and slow calcium current in dysgenic muscle by dihydropyridine receptor complementary DNA. *Nature*. 336: 134–139.
- Tareilus, E., M. Roux, N. Qin, R. Olcese, J. Zhou, E. Stefani, and L. Birnbaumer. 1997. A *Xenopus* oocyte β subunit. Evidence for a role in the assembly/expression of voltage-gated calcium channels that is separate from its role as a regulatory subunit. *Proc. Natl. Acad. Sci. USA*. 94:1703–1708.
- Wei, X., E. Perez-Reyes, A. E. Lacerda, G. Schuster, M. A. Brown, and L. Birnbaumer. 1991. Heterologous regulation of the cardiac Ca^{2+} channel $\alpha 1$ subunit by skeletal muscle β and γ subunits. *J. Biol. Chem.* 266:21943–21947.